

Novel Oxadiazole Analogues Derived from Ethacrynic Acid: Design, Synthesis, and Structure–Activity Relationships in Inhibiting the Activity of Glutathione *S*-Transferase P1-1 and Cancer Cell Proliferation

Xinmei Yang,[†] Guyue Liu,[‡] Hongcai Li,[†] Yun Zhang,[†] Dandan Song,[‡] Chunmin Li,[†] Rui Wang,[§] Bo Liu,[†] Wen Liang,[†] Yongkui Jing,[§] and Guisen Zhao^{*†}

[†]*School of Pharmaceutical Sciences, Shandong University, Jinan, Shandong 250012, P. R. China*, [‡]*Shenyang Pharmaceutical University, Shenyang 110016, P. R. China*, and [§]*Mount Sinai School of Medicine, One Gustave L. Levy Place, New York, New York 10029*

Received August 4, 2009

Ethacrynic acid (EA) is a glutathione *S*-transferase P1-1 (GST P1-1) inhibitor with weak antiproliferative ability in tumor cells. By use of the principle of bioisosterism, a series of novel EA oxadiazole analogues were designed and synthesized. The structure–activity relationships of inhibiting GST P1-1 activity and cell proliferation of those EA analogues were investigated in human leukemia HL-60 cells. Our data revealed that those EA oxadiazole analogues had improved antiproliferative activity and most of them had similar or better inhibitory effects on GST P1-1 activity than EA. Compound **6u** was one of the potent antiproliferative agents without inhibition of GST P1-1 activity. Compounds **6r** and **6s** were two potent cell growth inhibitors in several solid tumor cell lines with the concentrations inhibiting half of cell growth of less than 5 μ M. Our data suggest that these EA oxadiazole analogues are promising antitumor agents that may act through GST P1-1 inhibition-dependent and/or -independent pathways.

Introduction

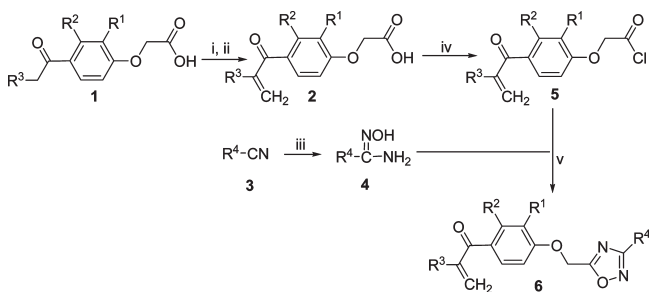
Glutathione *S*-transferases (GSTs), a family of phase II detoxification enzymes, play an important role in the protection of cells from injury by toxic chemical including some chemotherapeutic agents through catalyzing conjugation with glutathione.¹ Among these enzymes, glutathione *S*-transferase P1-1 (GST P1-1^a) is the predominant isozyme of this family and has been found to overexpress in a number types of human cancers including stomach carcinoma, colon cancer, pancreatic cancer, and lung cancer.^{2,3} The increased levels of GST P1-1 have been found to be relevant to the development of resistance toward chemotherapeutic agents by catalyzing their conjugation with glutathione (GSH) to form either inactivated conjugates or conjugates that can be easily effluxed.⁴ In addition, GST P1-1 has been shown to decrease the levels of hydrogen peroxide by promoting its catabolism and to protect against hydrogen peroxide-induced cell death.^{5,6} Hydrogen peroxide is one member of reactive oxygen species (ROS) that play important roles in regulating cell proliferation, apoptosis, and senescence.⁷ Recently it was found that GST P1-1 acted as an endogenous inhibitor that suppresses the activation of c-Jun N-terminal kinase (JNK) through a noncatalytic protein–protein interaction and protects cells against stress-induced apoptosis.^{7,8} JNK is a member of the

mitogen activated stress kinase (MAPK) family, which mediates many important pathways in the transduction of cell survival and apoptotic signals initiated by stress or toxic stimuli.⁸ Considering the multiple functions of GST P1-1 in regulating multidrug resistance (MDR), cell proliferation, and apoptosis, it has been considered as a target for developing therapeutic agents for cancer treatment.^{9,10}

Ethacrynic acid (EA) is a known GST P1-1 inhibitor with an α,β -unsaturated carbonyl functional group.^{11,12} EA by itself inhibits tumor cell growth at high concentrations, and it enhances the therapeutic efficiencies of several anticancer agents.¹³ The low efficacy and side effects of EA limit its clinical use.^{14,15} It has been found that the ability of EA to inhibit GST P1-1 activity results from its α,β -unsaturated carbonyl group and that the main diuretic side effect of EA results from its carboxyl group.¹⁶ We have done structure modifications of EA and found that EA derivatives with double substitutions on the phenyl cycle together with the α,β -unsaturated carbonyl group were required to maintain GST P1-1 activity inhibition and cell growth inhibition ability.^{17,18} Moreover, we found that EA esters, such as EA butyl ester, have increased cell growth inhibitory ability significantly.^{18,19} These esters are unstable *in vivo* and can be metabolized rapidly to EA.¹⁹ The similarities of electrolyte and conformational properties as well as the physicochemical properties such as pK_a and $\log P$ of EA denote that an authentic bioisosteric relationship exists between the ester (CO₂R)– and heterocyclic oxadiazole-containing analogues.²⁰ On the basis of the bioisosterism principle, we designed and synthesized 28 novel EA derivatives containing a heterocyclic oxadiazole. The inhibitory effects of these compounds on GST P1-1 activity in HL-60 cell lysates and on HL-60 cell proliferation were determined. The relationship between GST

*To whom correspondence should be addressed. Phone: +86 531 88382009. Fax: +86 531 88382835. E-mail: guisenzhao@sdu.edu.cn.

^a Abbreviations: CDNB, 1-chloro-2,4-dinitrobenzene; EA, ethacrynic acid; EGF, epidermal growth factor; FBS, fetal bovine serum; GSH, glutathione; GST P1-1, glutathione *S*-transferase P1-1; HPLC, high performance liquid chromatography; JNK, c-jun N-terminal kinase; MAPK, mitogen-activated protein kinase; MDR, multidrug resistance; MTT, 3-(4,5-dimethylthiazol-2-yl)-2,5-diphenyltetrazolium bromide; ROS, reactive oxygen species; SAR, structure–activity relationship.

Scheme 1. Synthetic Routes of Target Compounds^a

^a Reagents and conditions: (i) paraformaldehyde, dimethylamine hydrochloride, HAc, 100 °C; (ii) 10% NaHCO₃ (aq), reflux, HCl; (iii) NH₂OH·HCl, K₂CO₃, alcohol, reflux; (iv) SOCl₂, toluene, 90–100 °C; (v) pyridine, 100 °C.

P1-1 activity inhibition and the antiproliferative abilities was analyzed. Compounds **6r** and **6s** were two of the most effective inhibitors on HL-60 cell growth with the ability to inhibit GST P1-1 activity. The antiproliferative effects of both compounds **6r** and **6s** were determined in additional cancer cell lines including two prostate cancer cell lines, PC-3 and DU145, three breast cancer cell lines, T47D, MCF-7, and MDA-MB-231, and one nontumorigenic epithelial cell line, MCF 10A.

Chemistry

The schematic pathways of synthesizing α,β -unsaturated carbonyl EA analogues containing a heterocyclic oxadiazole are shown in Scheme 1. The starting material compounds **1** were prepared from the appropriate phenol in two steps as we previously described.¹⁷ Compounds **1** with paraformaldehyde and dimethylamine hydrochloride in the presence of a catalytic amount of acetic acid gave Mannich compounds which were then converted to compounds **2** under alkaline condition via an elimination reaction.²¹ EA was obtained from the commercial source (TCI, Tokyo Kasei Kogyo Co., Ltd.). Acyl chlorides **5** were produced from compounds **2** using thionyl chloride as a chlorinating agent and toluene as the solvent. The reaction mixture was refluxed for 4 h and then cooled to room temperature. After evaporation under reduced pressure to remove toluene, the obtained acyl chlorides **5** were used in the next step without further purification.

The key intermediates, amidoximes **4**, were synthesized from the corresponding nitrile. Suitable nitriles **3** in an alcoholic solution containing hydroxylamine hydrochloride and anhydrous potassium carbonate were heated to reflux for 4–16 h. Filtration and purification on silica gel chromatography afforded good yields of compounds **4**.²²

The target compounds, 1,2,4-oxadiazoles **6**, were obtained from compounds **4** and compounds **5** by cyclization of *O*-acylamidoximes according to a reported method.²³ Flash column chromatography, eluting with different proportions of petroleum ether–acetone, gave pure types of compounds **6**.

The R⁴-group of intermediates of compounds **4** was used as a handle to introduce structural diversity. A substitutive benzene ring was introduced at this position in most of these compounds.

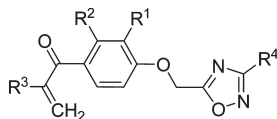
Results and Discussion

The structures of α,β -unsaturated carbonyl EA analogues containing a heterocyclic oxadiazole prepared in this study are shown in Table 1. The inhibition of these compounds on GST P1-1 activity in HL-60 cell lysate was investigated in vitro as

previously described.¹⁸ Cell growth inhibition ability was determined by counting cells with the aid of a hemocytometer, and the concentrations that inhibit growth of HL-60 cells by 50% (GI₅₀) were determined.

Substituents of those lead compounds are shown in Table 1. From the results obtained, it was noticed that all compounds in this series, except compound **6u**, inhibited GST P1-1 activity with effects comparable to or better than EA. The most potent compounds in inhibiting the activity of GST P1-1 were compounds **6o**, **6p**, and **6q**. The influences of the substituents chlorine, bromide, or methyl on the middle phenyl group on the GST P1-1 activity inhibition were analyzed. Compounds with one chlorine substitution (**6n–q**) at the R²-position of the phenyl ring inhibited GST P1-1 better than compounds containing one methyl substitution (**6a–f**) or one bromide substitution (**6y**, **6z**, **6aa**, and **6ab**) at the same position. Compounds with double chlorine substitutions (**6r–s**) at the R²- and R¹- positions of the phenyl ring inhibited GST P1-1 poorly than compounds containing one chlorine substitution (**6n–q**). The influences of substituents at the oxadiazole ring on abilities of inhibiting GST P1-1 activity were also analyzed. Compounds substituted with a phenyl group at the R⁴-position on the oxadiazole ring were more potent GST P1-1 activity inhibitors than those with one methyl substitution. Among compounds **6h–m**, those containing either electron-withdrawing or electron-donating para-substituent groups (e.g., NO₂, MeO, CF₃, and F) at the phenyl ring (**6i–m**) had less ability in inhibiting GST P1-1 activity than the compound (**6h**) containing unsubstituted benzene at the R⁴-position. It has been shown that EA inhibits the GST P1-1 activity by binding to GST P1-1 through the α,β -unsaturated carbonyl group.^{12,24} All our synthesized compounds kept the α,β -unsaturated carbonyl group and exhibited the ability to inhibit GST P1-1 activity except compound **6u**. Our results suggest that additional reactions may be needed for GST P1-1 activity inhibition and those compounds with or without the ability to inhibit GST P1-1 activity could be used as lead molecules to dissect the relationship between the GST P1-1 binding and activity inhibition.

Although those lead compounds had slight improvement on the GST P1-1 activity inhibition, they exhibited much more improved antiproliferative activities over EA in HL-60 cells (Table 1). Our principle is to use a heterocyclic oxadiazole to replace the ester (CO₂R)– for improving the antiproliferative ability of EA based on an authentic bioisosteric relationship existing between the ester (CO₂R)– and the heterocyclic oxadiazole-containing analogues. The antiproliferative data shown here support this principle. EA analogues containing a heterocyclic oxadiazole have similar cell growth inhibition abilities with that of the EA esters.¹⁸ Structure–activity analysis of those oxadiazole-containing analogues on cell growth inhibition indicated that substituents at the end phenyl group of the oxadiazole ring did not influence cell growth inhibition. Trifluoromethyl substituents showed a modest improvement in HL-60 cell growth inhibition (e.g., **6k**, **6q**, **6u**, and **6ab**) with GI₅₀ < 2.0 μ M that was 20-fold more active than the lead compound, EA. It is unclear whether the antiproliferative effects of EA and its derivatives are mediated through GST P1-1 activity inhibition. The glutathione conjugates of EA and its esters have increased ability in inhibiting GST P1-1 activity.^{24,25} However, they were not effective, or less effective, in inhibiting tumor cell growth.¹⁹ EA and its derivatives form conjugates with GSH both spontaneously and by GST-driven catalysis, and the α,β -unsaturated carbonyl moiety of EA is

Table 1. Substituents of Synthesized EA Analogues Containing an Oxadiazole Group and Their Inhibitory Effects on GST P1-1 Activity and Proliferation of HL-60 Cells

compd	R ¹	R ²	R ³	R ⁴	IC ₅₀ (μM) for inhibiting GST P1-1 activity ^a	GI ₅₀ (μM) for inhibiting HL-60 cell growth ^b
EA	Cl	Cl	C ₂ H ₅	-	3.4 ± 0.7	45.0 ± 1.1
6a	H	CH ₃	CH ₃	CH ₃	5.0 ± 2.0	3.82
6b	H	CH ₃	CH ₃	phenyl	1.97 ± 0.3	6.7 ± 3.0
6c	H	CH ₃	CH ₃	4-OH phenyl	2.1 ± 1.1	3.5 ± 0.8
6d	H	CH ₃	CH ₃	4-F phenyl	3.5 ± 1.3	4.6 ± 0.9
6e	H	CH ₃	CH ₃	4-CF ₃ phenyl	3.3 ± 0.6	3.2 ± 0.8
6f	H	CH ₃	CH ₃	4-NO ₂ benzyl	2.9 ± 0.1	6.1 ± 3.6
6g	CH ₃	CH ₃	CH ₃	CH ₃	4.0 ± 1.0	3.2 ± 0.4
6h	CH ₃	CH ₃	CH ₃	phenyl	1.8 ± 0.9	3.5 ± 0.6
6i	CH ₃	CH ₃	CH ₃	4-OH phenyl	3.4 ± 1.1	3.5 ± 0.5
6j	CH ₃	CH ₃	CH ₃	4-F phenyl	2.4 ± 0.6	2.1 ± 0.6
6k	CH ₃	CH ₃	CH ₃	4-CF ₃ phenyl	3.9 ± 0.4	1.4 ± 0.5
6l	CH ₃	CH ₃	CH ₃	4-Cl benzyl	2.0 ± 0.5	3.1 ± 0.7
6m	CH ₃	CH ₃	CH ₃	4-NO ₂ benzyl	2.3 ± 0.5	2.4 ± 0.7
6n	H	Cl	CH ₃	CH ₃	2.1 ± 0.6	9.7 ± 1.6
6o	H	Cl	CH ₃	phenyl	0.6 ± 0.1	5.4 ± 1.5
6p	H	Cl	CH ₃	4-F phenyl	0.7 ± 0.5	2.8 ± 0.8
6q	H	Cl	CH ₃	4-CF ₃ phenyl	0.7 ± 0.1	1.9 ± 0.5
6r	Cl	Cl	C ₂ H ₅	CH ₃	4.0 ± 0.3	2.3 ± 0.2
6s	Cl	Cl	C ₂ H ₅	phenyl	3.6 ± 0.7	1.7 ± 0.1
6t	Cl	Cl	C ₂ H ₅	4-F phenyl	3.9 ± 0.8	1.7 ± 1.0
6u	Cl	Cl	C ₂ H ₅	4-CF ₃ phenyl	> 40	1.1 ± 0.2
6v	Cl	Cl	C ₂ H ₅	4-OCH ₃ phenyl	3.8 ± 1.2	1.5 ± 0.3
6w	Cl	Cl	C ₂ H ₅	4-Cl benzyl	5.4 ± 2.0	1.6 ± 0.3
6x	Cl	Cl	C ₂ H ₅	4-NO ₂ benzyl	3.3 ± 0.6	1.6 ± 0.2
6y	H	Br	CH ₃	CH ₃	3.2 ± 1.3	3.2 ± 0.7
6z	H	Br	CH ₃	phenyl	2.0 ± 0.5	7.9 ± 1.7
6aa	H	Br	CH ₃	4-F phenyl	1.4 ± 0.5	3.2 ± 0.8
6ab	H	Br	CH ₃	4-CF ₃ phenyl	1.3 ± 0.3	1.7 ± 0.7

^aIC₅₀ indicates the concentration of the tested compound that inhibits 50% of GST P1-1 activity. ^bGI₅₀ indicates the concentration of the tested compound that inhibits 50% of HL-60 cell growth.

the target for conjugation.²⁶ GSH is a major regulator of the redox equilibrium and protects against mitochondrial-mediated apoptosis.²⁷ The depletion and reduction of GSH increases the sensitivity of cells to toxic insults by regulating the apoptosis-associated redox potential and by inducing changes in mitochondrial function.²⁸ EA and EA derivatives depleted intracellular GSH which was correlated with their antitumor activity.¹⁹ Recently it has been shown that EA and its derivatives inhibited the signaling pathways of NF-κB and Wnt/β-catenin signaling through covalently modifying sulfhydryl groups.^{29,30} Reduction of the α,β-unsaturated carbonyl group abrogated the inhibition on the Wnt/β-catenin signaling.³⁰ These data suggest that the antiproliferative effects of EA and its derivatives including the compounds described here may inhibit cell growth through a GST P1-1 inhibition-independent pathway due to their binding to GSH or the thiol groups of functional proteins. Compound **6u** containing the α,β-unsaturated carbonyl group without the ability of inhibiting GST P1-1 ability supports this expectation.

Compounds **6r** and **6s** have the same substituents as EA esters in R¹, R², and R³ positions and are two of the most effective EA oxadiazole-containing analogues in inhibiting HL-60 cell growth (Table 1). The growth inhibitory effects of

Table 2. Growth Inhibitory Effects of **6r** and **6s** in Several Solid Tumor Cell Lines

cell lines	GI ₅₀ (μM) ^a	
	6r	6s
PC-3	1.4 ± 0.2	1.5 ± 0.1
DU145	2.1 ± 0.2	3.7 ± 0.3
T47D	2.0 ± 0.2	2.6 ± 0.2
MCF-7	1.6 ± 0.1	2.0 ± 0.2
MDA-MB-231	4.0 ± 0.2	4.5 ± 0.3
MCF-10A	5.0 ± 0.4	5.9 ± 0.7

^aCell growth inhibition was determined using the MTT assay. Cells were treated with various concentrations of **6r** and **6s** for 4 days, and GI₅₀ was calculated. The data shown are the mean ± SD of three independent experiments.

both compounds in additional cancer cell lines were investigated (Table 2). Our data showed that PC-3, DU-145, T47D, and MCF-7 cells were more sensitive than nontumorigenic MCF 10A cells to the treatment of both agents.

Conclusion

By use of the principle of bioisosterism, α,β-unsaturated carbonyl EA analogues containing a heterocyclic oxadiazole

were synthesized. On the basis of their inhibitory effects on GST P1-1 activity and HL-60 cell growth, it was revealed that (1) the replacement of the carboxyl group by an oxadiazole group in the structure of EA improved its antiproliferative ability more efficiently than previously published carboxylic acid and ester derivatives¹⁸ and (2) most of those compounds had similar or better inhibitory effects on GST P1-1 activity as EA. Some of those compounds may inhibit cell proliferation independent of GST P1-1 activity inhibition. The connection between GST P1-1 activity inhibition and cell growth inhibition of these compounds needs to be further investigated. We anticipate that these analogues represent a new group of antitumor candidates.

Experimental Section

Unless otherwise noted, all materials were obtained from commercial suppliers and used without further purification. All melting points were determined in a Büchi capillary melting point apparatus and are uncorrected. The infrared (IR) spectra were measured on KBr pellets using a Nicolet Nexus 470FT-IR spectrometer and were expressed in cm^{-1} . The proton nuclear magnetic resonance (^1H NMR) spectra were recorded with a Bruker Avance DRX600 instrument with tetramethylsilane (TMS) as the internal standard. The chemical shifts (δ) were reported in parts per million (ppm) and were relative to the central peak of the solvent, which was DMSO- d_6 or CDCl_3 . Coupling constants (J) were given in Hz. Data were reported as follows: chemical shift, multiplicity (s = singlet, d = doublet, t = triplet, q = quartet, br = broad, m = multiplet), coupling constants, and number of protons. Mass spectra (MS) were measured with an API 4000, and the high resolution mass spectra data were obtained using a Accela UPLC-LTQ Orbitrap mass spectrometer. Column chromatography was carried out with silica gel in the solvents indicated. Thin-layer chromatography (TLC) was performed on silica gel GF254 plates (layer thickness, 0.2 mm), and compounds were visualized using UV light. Petroleum ether used for TLC and column chromatography had a boiling range of 60–90 °C. All tested compounds were more than 95% pure on the basis of HPLC analysis. The specific method for HPLC analysis and a table of the data for all tested compounds are in Supporting Information.

Synthesis of the Compound 2 Series. The starting materials **1** were synthesized via methods reported previously.¹⁷ In a 50 mL round-bottomed flask equipped with an outlet tube suitable for application of intermittent suction, an intimate mixture of **1** (9.6 mmol), paraformaldehyde (0.38 g, 11.5 mmol), dimethylamine hydrochloride (0.91 g, 10.4 mmol), and acetic acid (0.05 mL) was heated to 100 °C for about 1.5 h, during which period suction was applied. When the mixture was cooled to room temperature, the Mannich compounds obtained were dissolved in 10% sodium bicarbonate and modulated to slight alkalinity. The resulting solution was heated to 100 °C for 0.5 h, cooled, and acidified using concentrated hydrochloric acid. The products obtained were filtered and dried. The crude products were purified by column chromatography by eluting with acetone/petroleum ether (1:3). The parameters of compounds **2** were as follows.

[3-Methyl-4-(2-methylene-1-oxopropyl)phenoxy]acetic Acid (2a). White powder, yield 83.5%, mp 112.1–114.1 °C, TLC R_f = 0.22 (acetone/petroleum ether, 1:3, v/v). ^1H NMR (DMSO- d_6) δ (ppm): 7.25 (d, J = 8.47 Hz, 1H), 6.79 (d, J = 2.36 Hz, 1H), 6.68 (dd, J_1 = 2.54 Hz, J_2 = 8.48 Hz, 1H), 5.99 (s, 1H), 5.44 (s, 1H), 4.72 (s, 2H), 2.23 (s, 3H), 1.94 (s, 3H). HRMS (ESI) m/z calcd for $\text{C}_{13}\text{H}_{15}\text{O}_4$ [M + H]⁺: 235.0965, found 235.0953.

[2,3-Dimethyl-4-(2-methylene-1-oxopropyl)phenoxy]acetic Acid (2b). White powder, yield 74.5%, mp 119.5–121.3 °C, TLC R_f = 0.38 (acetone/petroleum ether, 1:2, v/v). ^1H NMR (DMSO- d_6) δ (ppm): 13.0 (s, 1H), 7.05 (d, J = 8.40 Hz, 1H), 6.74 (d,

J = 9.00 Hz, 1H), 6.02 (s, 1H), 5.46 (s, 1H), 4.73 (s, 2H), 2.15 (s, 3H), 2.10 (s, 3H), 1.95 (s, 3H). HRMS (ESI) m/z calcd for $\text{C}_{14}\text{H}_{17}\text{O}_4$ [M + H]⁺: 249.1121, found 249.1108.

[3-Chloro-4-(2-methylene-1-oxopropyl)phenoxy]acetic Acid (2c). White powder, yield 34.3%, mp 107.4–109.5 °C, TLC R_f = 0.45 (acetone/petroleum ether, 1:3, v/v). ^1H NMR (DMSO- d_6) δ (ppm): 7.33 (d, J = 8.53 Hz, 1H), 7.10 (d, J = 2.44 Hz, 1H), 6.97 (dd, J_1 = 2.45 Hz, J_2 = 8.50 Hz, 1H), 6.10 (s, 1H), 5.51 (s, 1H), 4.80 (s, 2H), 1.94 (s, 3H). HRMS (ESI) m/z calcd for $\text{C}_{12}\text{H}_{12}\text{O}_4\text{Cl}$ [M + H]⁺: 255.0419, found 255.0406.

[3-Bromo-4-(2-methylene-1-oxopropyl)phenoxy]acetic Acid (2d). White powder, yield 28.3%, mp 123.5–124.4 °C, TLC R_f = 0.44 (acetone/petroleum ether, 1:2, v/v). ^1H NMR (DMSO- d_6) δ (ppm): 13.15 (s, 1H), 7.32 (d, J = 9.00 Hz, 1H), 7.10 (d, J = 1.80 Hz, 1H), 7.02 (dd, J_1 = 2.40 Hz, J_2 = 8.40 Hz, 1H), 6.11 (s, 1H), 5.50 (s, 1H), 4.80 (s, 2H), 1.94 (s, 3H). HRMS (ESI) m/z calcd for $\text{C}_{12}\text{H}_{12}\text{O}_4\text{Br}$ [M + H]⁺: 298.9913, found 298.9901.

Synthesis of the Compound 4 Series. Hydroxylamine hydrochloride (50 mmol) and anhydrous potassium carbonate (50 mmol) were dissolved in 40 mL of dry alcohol and stirred for 0.5 h at room temperature. The corresponding nitriles (10 mmol) **3** were added, and the reaction mixture was heated to reflux for 4–16 h. After filtration of inorganic salts, the solvent was evaporated under reduced pressure. The products **4** were purified by column chromatography (petroleum ether/acetone, 2:1, v/v).

***N*-Hydroxyacetimidamide (4a).** White crystalline solid, yield 56.5%, mp 136.3–137.7 °C. ^1H NMR (CDCl_3) δ (ppm): 8.66 (s, 1H), 5.34 (s, 2H), 1.61 (s, 3H).

***N*-Hydroxybenzimidamide (4b).** White crystalline solid, yield 55.8%, mp 72.1–73.2 °C, TLC R_f = 0.35 (acetone/petroleum ether, 1:2, v/v). ^1H NMR (CDCl_3) δ (ppm): 9.62 (s, 1H), 7.67 (m, 2H), 7.36 (m, 3H), 5.80 (s, 2H).

***N*-Hydroxy-4-hydroxybenzimidamide (4c).** Light-yellow crystalline solid, yield 55.0%, TLC R_f = 0.24 (acetone/petroleum ether, 1:1, v/v). ^1H NMR (DMSO- d_6) δ (ppm): 9.59 (s, 1H), 9.35 (s, 1H), 7.47 (d, J = 8.40 Hz, 2H), 6.72 (d, J = 9.00 Hz, 2H), 5.63 (s, 2H). MS (ESI) m/z : 158.2 [M + H]⁺.

4-Fluoro-*N*-hydroxybenzimidamide (4d). White crystalline solid, yield 56.5%, mp 79.4–80.1 °C, TLC R_f = 0.47 (acetone/petroleum ether, 1:1, v/v). ^1H NMR (DMSO- d_6) δ (ppm): 9.66 (s, 1H), 7.71 (m, 2H), 7.20 (m, 2H), 5.84 (s, 2H).

***N*-Hydroxy-4-(trifluoromethyl)benzimidamide (4e).** White crystalline solid, yield 86.0%, mp 94.7–95.3 °C, TLC R_f = 0.57 (acetone/petroleum ether, 1:1, v/v). ^1H NMR (DMSO- d_6) δ (ppm): 9.92 (s, 1H), 7.89 (d, J = 7.80 Hz, 2H), 7.74 (d, J = 8.40 Hz, 2H), 5.98 (s, 2H).

2-(4-Chlorophenyl)-*N*-hydroxyacetimidamide (4f). White crystalline solid, yield 54.8%, mp 92.3–93.0 °C, TLC R_f = 0.51 (acetone/petroleum ether, 1:1, v/v). ^1H NMR (DMSO- d_6) δ (ppm): 8.91 (s, 1H), 7.33 (d, J = 8.40 Hz, 2H), 7.28 (d, J = 8.40 Hz, 2H), 5.43 (s, 2H), 3.24 (s, 2H). MS (ESI) m/z : 184.6 [M + H]⁺.

***N*-Hydroxy-2-(4-nitrophenyl)acetimidamide (4g).** Light-yellow crystalline solid, yield 90.0%, mp 166.2–166.9 °C, TLC R_f = 0.34 (acetone/petroleum ether, 1:1, v/v). ^1H NMR (DMSO- d_6) δ (ppm): 9.01 (s, 1H), 8.16 (d, J = 9.00 Hz, 2H), 7.28 (d, J = 9.00 Hz, 2H), 5.43 (s, 2H), 3.42 (s, 2H). MS (ESI) m/z : 195.9 [M + H]⁺.

***N*-Hydroxy-4-methoxybenzimidamide (4h).** White crystalline solid, yield 57.5%, mp 123.6–124.2 °C, TLC R_f = 0.48 (acetone/petroleum ether, 1:1, v/v). ^1H NMR (DMSO- d_6) δ (ppm): 9.46 (s, 1H), 7.61 (d, J = 9.00 Hz, 2H), 6.92 (d, J = 9.00 Hz, 2H), 5.74 (s, 2H), 3.76 (s, 3H).

Synthesis of the Compound 5 Series. To a suspension of **2** (2 mmol) in anhydrous toluene (10 mL) was added thionyl chloride (0.15 mL, 2 mmol). The reaction mixture was refluxed for 4 h and then cooled to room temperature. The resulting solution of **5** in toluene was suitable for use without further purification.

Synthesis of the Target Compounds of the 6 Series. A solution of **5** (2 mmol) in toluene (10 mL) was added dropwise to a

solution of amidoximes **4** (2 mmol) in pyridine (5 mL). The mixture was stirred at 100 °C for about 1 h. The supernatant fluid was decanted, and the residue was washed with CH₂Cl₂. The combined organic solvent phase was evaporated at reduced pressure to yield the crude product which was purified by flash chromatography with acetone/petroleum ether (1:3) and acetone/petroleum ether (1:6) to give **6**.

5-[3-Methyl-4-(2-methylene-1-oxopropyl)phenoxyethyl]-3-methyl-1,2,4-oxadiazole (6a). Yellow powder, yield 57.0%, mp 60.3–61.5 °C, TLC R_f = 0.61 (acetone/petroleum ether, 1:3, v/v). ¹H NMR (CDCl₃) δ (ppm): 7.28 (d, J = 8.30 Hz, 1H), 6.86 (s, 1H), 6.79 (d, J = 8.42 Hz, 1H), 5.92 (s, 1H), 5.55 (s, 1H), 5.28 (s, 2H), 2.45 (s, 3H), 2.33 (s, 3H), 2.04 (s, 3H). IR (KBr, cm⁻¹): ν_{CH} , 3060.52; ν_{CH} , 2978.06, 2954.75, 2924.05; $\nu_{\text{C=O}}$, 1644.31; $\nu_{\text{C=C}}$, 1605.92; $\nu_{\text{C-O}}$, 1249.34; γ_{CH_2} , 1131.81, 803.12. HRMS (ESI) m/z calcd for C₁₅H₁₇N₂O₃ [M + H]⁺: 273.2866, found 273.2871.

5-[3-Methyl-4-(2-methylene-1-oxopropyl)phenoxyethyl]-3-phenyl-1,2,4-oxadiazole (6b). White powder, yield 51.3%, mp 56.7–57.9 °C, TLC R_f = 0.42 (acetone/petroleum ether, 1:3, v/v). ¹H NMR (CDCl₃) δ (ppm): 8.09 (d, J = 7.80 Hz, 2H), 7.51 (m, 3H), 7.28 (d, J = 8.40 Hz, 1H), 6.89 (s, 1H), 6.83 (d, J = 8.40 Hz, 1H), 5.92 (s, 1H), 5.55 (s, 1H), 5.37 (s, 2H), 2.33 (s, 3H), 2.03 (s, 3H). IR (KBr, cm⁻¹): ν_{CH} , 3088.19, 3076.41; ν_{CH} , 2955.08, 2922.63; $\nu_{\text{C=O}}$, 1646.10; $\nu_{\text{C=C}}$, 1605.92; $\nu_{\text{C-O}}$, 1242.07; γ_{CH_2} , 1126.13, 717.16, 693.14. HRMS (ESI) m/z calcd for C₂₀H₁₉N₂O₃ [M + H]⁺: 335.1390, found 335.1394.

5-[3-Methyl-4-(2-methylene-1-oxopropyl)phenoxyethyl]-3-(4-hydroxyphenyl)-1,2,4-oxadiazole (6c). White powder, yield 45.3%, mp 123.3–123.9 °C, TLC R_f = 0.30 (acetone/petroleum ether, 1:3, v/v). ¹H NMR (CDCl₃) δ (ppm): 7.96 (d, J = 8.40 Hz, 2H), 7.28 (d, J = 8.40 Hz, 1H), 6.93 (d, J = 8.40 Hz, 2H), 6.88 (s, 1H), 6.82 (d, J = 8.40 Hz, 1H), 6.28 (s, 1H), 5.94 (s, 1H), 5.57 (s, 1H), 5.34 (s, 2H), 2.33 (s, 3H), 2.04 (s, 3H). ¹³C NMR (CDCl₃) δ (ppm): 200.26, 174.20, 168.28, 158.78, 158.62, 145.28, 139.58, 132.67, 130.68, 129.49, 129.43, 118.49, 117.38, 115.95, 110.82, 60.92, 20.30, 17.62. IR (KBr, cm⁻¹): ν_{OH} , 3293.53; ν_{CH} , 2957.00, 2924.12; $\nu_{\text{C=O}}$, 1641.16; $\nu_{\text{C=C}}$, 1602.60, 1584.13; δ_{CH} , 1481.33, 1447.80, 1347.23; $\nu_{\text{C-O}}$, 1225.23, 1078.11; γ_{CH_2} , 844.93, 752.98. HRMS (ESI) m/z calcd for C₂₀H₁₉N₂O₄ [M + H]⁺: 351.1339, found 351.1345.

5-[3-Methyl-4-(2-methylene-1-oxopropyl)phenoxyethyl]-3-(4-fluorophenyl)-1,2,4-oxadiazole (6d). White powder, yield 64.5%, mp 73.2–74.0 °C, TLC R_f = 0.41 (acetone/petroleum ether, 1:4, v/v). ¹H NMR (CDCl₃) δ: 8.10 (m, 2H), 7.28 (m, 1H), 7.18 (m, 2H), 6.89 (s, 1H), 6.83 (m, 1H), 5.92 (s, 1H), 5.55 (s, 1H), 5.37 (s, 2H), 2.34 (s, 3H), 2.04 (s, 3H). ¹³C NMR (CDCl₃) δ (ppm): 199.62, 174.57, 167.81, 164.72 (d, $J_{\text{C-F}}$ = 250.65 Hz), 158.47, 145.32, 139.55, 132.88, 130.59, 129.74 (d, $J_{\text{C-F}}$ = 9.15 Hz), 129.01, 122.48 (d, $J_{\text{C-F}}$ = 3.3 Hz), 117.33, 116.16 (d, $J_{\text{C-F}}$ = 21.75 Hz), 110.75, 60.88, 20.29, 17.61. IR (KBr, cm⁻¹): ν_{CH} , 3057.09; ν_{CH} , 2968.63, 2930.51, 2858.33; $\nu_{\text{C=O}}$, 1642.69; $\nu_{\text{C=C}}$, 1622.13, 1607.41, 1586.18; δ_{CH} , 1485.45, 1420.06, 1355.35; $\nu_{\text{C-O}}$, 1241.51, 1016.44; γ_{CH_2} , 964.64, 856.83, 803.66, 754.22. HRMS (ESI) m/z calcd for C₂₀H₁₈FN₂O₃ [M + H]⁺: 353.1296, found 353.1300.

5-[3-Methyl-4-(2-methylene-1-oxopropyl)phenoxyethyl]-3-(4-trifluoromethylphenyl)-1,2,4-oxadiazole (6e). White powder, yield 66.4%, mp 87.9–88.8 °C, TLC R_f = 0.48 (acetone/petroleum ether, 1:3, v/v). ¹H NMR (CDCl₃) δ (ppm): 8.23 (d, J = 8.40 Hz, 2H), 7.76 (d, J = 7.80 Hz, 2H), 7.29 (d, J = 8.40 Hz, 1H), 6.90 (d, J = 7.80 Hz, 1H), 6.84 (m, 1H), 5.93 (s, 1H), 5.55 (s, 1H), 5.39 (s, 2H), 2.34 (s, 3H), 2.04 (s, 3H). ¹³C NMR (CDCl₃) δ (ppm): 199.61, 175.02, 167.66, 158.43, 145.35, 139.58, 133.32, 130.59, 129.64, 129.02, 127.94, 125.95 (q, $J_{\text{C-F}}$ = 3.80 Hz), 124.60, 122.80, 117.35, 110.77, 60.89, 20.29, 17.60. IR (KBr, cm⁻¹): ν_{CH} , 3069.12; ν_{CH} , 2966.74, 2926.34; $\nu_{\text{C=O}}$, 1640.08; $\nu_{\text{C=C}}$, 1624.44, 1610.78, 1571.70; δ_{CH} , 1451.65, 1421.08, 1328.32; $\nu_{\text{C-O}}$, 1247.66, 1067.29; γ_{CH_2} , 980.34, 853.44. HRMS (ESI) m/z calcd for C₂₁H₁₈F₃N₂O₃ [M + H]⁺: 403.1264, found 403.1270.

5-[3-Methyl-4-(2-methylene-1-oxopropyl)phenoxyethyl]-3-(4-nitrobenzyl)-1,2,4-oxadiazole (6f). White powder, yield 47.9%, mp 55.8–56.7 °C, TLC R_f = 0.33 (acetone/petroleum ether, 1:3, v/v). ¹H NMR (CDCl₃) δ (ppm): 8.20 (m, 2H), 7.51 (m, 2H), 7.26 (m, 1H), 6.83 (m, 1H), 6.77 (m, 1H), 5.93 (s, 1H), 5.53 (s, 1H), 5.28 (s, 2H), 4.23 (s, 2H), 2.31 (s, 3H), 2.04 (s, 3H). ¹³C NMR (CDCl₃) δ (ppm): 199.59, 175.05, 168.54, 158.31, 147.30, 145.35, 142.34, 139.50, 133.00, 130.51, 130.00, 129.01, 123.99, 117.28, 110.73, 60.83, 32.04, 20.25, 17.58. IR (KBr, cm⁻¹): ν_{CH} , 3064.17; ν_{CH} , 2925.85; $\nu_{\text{C=O}}$, 1652.01; $\nu_{\text{C=C}}$, 1627.66, 1607.43, 1571.97; ν_{NO_2} , 1522.50, 1350.14; δ_{CH} , 1494.70, 1447.68, 1371.74; $\nu_{\text{C-O}}$, 1238.84, 1125.47; γ_{CH_2} , 979.84, 841.49, 797.17. HRMS (ESI) m/z calcd for C₂₁H₂₀N₃O₅ [M + H]⁺: 394.1397, found 394.1401.

5-[2,3-Dimethyl-4-(2-methylene-1-oxopropyl)phenoxyethyl]-3-methyl-1,2,4-oxadiazole (6g). Yellow powder, yield 40.4%, mp 68.7–69.9 °C, TLC R_f = 0.58 (acetone/petroleum ether, 1:3, v/v). ¹H NMR (CDCl₃) δ (ppm): 7.08 (d, J = 8.42 Hz, 1H), 6.74 (d, J = 8.44 Hz, 1H), 5.95 (s, 1H), 5.58 (s, 1H), 5.29 (s, 2H), 2.46 (s, 3H), 2.24 (s, 3H), 2.20 (s, 3H), 2.05 (s, 3H). IR (KBr, cm⁻¹): ν_{CH} , 3097.90; ν_{CH} , 2984.24, 2954.83, 2925.30, 2861.81; $\nu_{\text{C=O}}$, 1656.36; $\nu_{\text{C=C}}$, 1592.41; $\nu_{\text{C-O}}$, 1295.77; γ_{CH_2} , 1086.35, 801.36. HRMS (ESI) m/z calcd for C₁₆H₁₉N₂O₃ [M + H]⁺: 287.1390, found 287.1394.

5-[2,3-Dimethyl-4-(2-methylene-1-oxopropyl)phenoxyethyl]-3-phenyl-1,2,4-oxadiazole (6h). White powder, yield 64.6%, mp 77.2–78.3 °C, TLC R_f = 0.47 (acetone/petroleum ether, 1:3, v/v). ¹H NMR (CDCl₃) δ (ppm): 8.09 (d, J = 6.60 Hz, 2H), 7.52 (m, 3H), 7.07 (d, J = 8.40 Hz, 1H), 6.78 (d, J = 8.40 Hz, 1H), 5.93 (s, 1H), 5.56 (s, 1H), 5.37 (s, 2H), 2.25 (s, 3H), 2.19 (s, 3H), 2.03 (s, 3H). IR (KBr, cm⁻¹): ν_{CH} , 2990.63, 2961.44, 2927.94, 2862.21; $\nu_{\text{C=O}}$, 1651.83; $\nu_{\text{C=C}}$, 1598.43; $\nu_{\text{C-O}}$, 1256.25; γ_{CH_2} , 1131.24, 721.53. HRMS (ESI) m/z calcd for C₂₁H₂₁N₂O₃ [M + H]⁺: 349.1547, found 349.1552.

5-[2,3-Dimethyl-4-(2-methylene-1-oxopropyl)phenoxyethyl]-3-(4-hydroxyphenyl)-1,2,4-oxadiazole (6i). White powder, yield 46.6%, mp 149.3–150.2 °C, TLC R_f = 0.27 (acetone/petroleum ether, 1:3, v/v). ¹H NMR (CDCl₃) δ (ppm): 7.96 (d, J = 9.00 Hz, 2H), 7.08 (d, J = 8.40 Hz, 1H), 6.91 (d, J = 8.40 Hz, 2H), 6.78 (d, J = 8.40 Hz, 1H), 6.00 (br, 1H), 5.96 (s, 1H), 5.59 (s, 1H), 5.34 (s, 2H), 2.24 (s, 3H), 2.19 (s, 3H), 2.05 (s, 3H). ¹³C NMR (CDCl₃) δ (ppm): 201.29, 174.47, 168.23, 158.63, 156.51, 145.49, 136.93, 133.79, 130.22, 129.38, 127.09, 126.42, 118.68, 115.92, 108.12, 61.52, 17.38, 17.23, 11.83. IR (KBr, cm⁻¹): ν_{OH} , 3269.34; ν_{CH} , 2928.45, 2861.80; $\nu_{\text{C=O}}$, 1629.63; $\nu_{\text{C=C}}$, 1616.22, 1599.31; δ_{CH} , 1484.13, 1434.40, 1355.00; $\nu_{\text{C-O}}$, 1260.27, 1083.12; γ_{CH_2} , 846.99, 753.37. HRMS (ESI) m/z calcd for C₂₁H₂₁N₂O₄ [M + H]⁺: 365.1496, found 365.1501.

5-[2,3-Dimethyl-4-(2-methylene-1-oxopropyl)phenoxyethyl]-3-(4-fluorophenyl)-1,2,4-oxadiazole (6j). White powder, yield 53.6%, mp 92.7–93.5 °C, TLC R_f = 0.57 (acetone/petroleum ether, 1:3, v/v). ¹H NMR (CDCl₃) δ (ppm): 8.10 (m, 2H), 7.18 (m, 2H), 7.08 (d, J = 8.40 Hz, 1H), 6.79 (d, J = 8.40 Hz, 1H), 5.94 (s, 1H), 5.57 (s, 1H), 5.37 (s, 2H), 2.25 (s, 3H), 2.20 (s, 3H), 2.04 (s, 3H). ¹³C NMR (CDCl₃) δ (ppm): 200.70, 174.88, 167.78, 164.72 (d, $J_{\text{C-F}}$ = 251.25 Hz), 156.40, 145.56, 136.94, 134.04, 129.73 (d, $J_{\text{C-F}}$ = 9.15 Hz), 129.69, 127.03, 126.36, 122.58 (d, $J_{\text{C-F}}$ = 2.85 Hz), 116.16 (d, $J_{\text{C-F}}$ = 21.75 Hz), 108.13, 61.50, 17.37, 17.20, 11.83. IR (KBr, cm⁻¹): ν_{CH} , 3066.30; ν_{CH} , 2985.69, 2956.57, 2923.40, 2870.25; $\nu_{\text{C=O}}$, 1645.28; $\nu_{\text{C=C}}$, 1607.26, 1594.56, 1583.07; δ_{CH} , 1483.45, 1455.92, 1357.80; $\nu_{\text{C-O}}$, 1261.62, 1080.80; γ_{CH_2} , 849.60, 792.73. HRMS (ESI) m/z calcd for C₂₁H₂₀FN₂O₃ [M + H]⁺: 367.1456, found 367.1452.

5-[2,3-Dimethyl-4-(2-methylene-1-oxopropyl)phenoxyethyl]-3-(4-trifluoromethylphenyl)-1,2,4-oxadiazole (6k). White powder, yield 55.9%, mp 123.6–124.2 °C, TLC R_f = 0.60 (acetone/petroleum ether, 1:3, v/v). ¹H NMR (CDCl₃) δ (ppm): 8.24 (d, J = 8.40 Hz, 2H), 7.77 (d, J = 8.40 Hz, 2H), 7.08 (d, J = 8.40 Hz, 1H), 6.79 (d, J = 9.00 Hz, 1H), 5.94 (s, 1H), 5.57 (s, 1H), 5.40

(s, 2H), 2.26 (s, 3H), 2.20 (s, 3H), 2.04 (s, 3H). ^{13}C NMR (CDCl_3) δ (ppm): 200.70, 175.30, 167.62, 156.33, 145.55, 136.98, 134.12, 133.29, 133.07, 129.77, 129.72, 127.92, 127.05, 126.34, 125.95 (q, $J_{\text{C-F}} = 3.70$ Hz), 108.13, 61.49, 17.36, 17.21, 11.84. IR (KBr, cm^{-1}): ν_{CH} , 2925.80; $\nu_{\text{C=O}}$, 1643.63; $\nu_{\text{C=C}}$, 1625.44, 1592.07, 1578.76; δ_{CH} , 1483.35, 1420.57, 1330.58; $\nu_{\text{C-O}}$, 1267.83, 1068.02; γ_{CH} , 850.64, 820.64, 758.75. HRMS (ESI) m/z calcd for $\text{C}_{22}\text{H}_{20}\text{F}_3\text{N}_2\text{O}_3$ [$\text{M} + \text{H}$] $^+$: 417.1421, found 417.1422.

5-[2,3-Dimethyl-4-(2-methylene-1-oxopropyl)phenoxyethyl]-3-(4-chlorobenzyl)-1,2,4-oxadiazol (6l). White powder, yield 51.3%, mp 54.5–55.4 °C, TLC $R_f = 0.52$ (acetone/petroleum ether, 1:3, v/v). ^1H NMR (CDCl_3) δ (ppm): 7.30 (d, $J = 8.40$ Hz, 2H), 7.26 (d, $J = 8.40$ Hz, 2H), 7.04 (d, $J = 9.00$ Hz, 1H), 6.70 (d, $J = 8.40$ Hz, 1H), 5.94 (s, 1H), 5.55 (s, 1H), 5.26 (s, 2H), 4.08 (s, 2H), 2.21 (s, 3H), 2.18 (s, 3H), 2.02 (s, 3H). ^{13}C NMR (CDCl_3) δ (ppm): 200.70, 174.97, 169.32, 156.27, 145.52, 136.89, 133.99, 133.52, 133.24, 130.37, 129.75, 128.92, 126.99, 126.28, 108.09, 61.46, 31.62, 17.36, 17.18, 11.80. IR (KBr, cm^{-1}): ν_{CH} , 2982.16, 2923.62; $\nu_{\text{C=O}}$, 1644.29; $\nu_{\text{C=C}}$, 1624.15, 1591.60, 1579.26; δ_{CH} , 1491.43, 1448.66, 1366.13; $\nu_{\text{C-O}}$, 1264.92, 1096.68; γ_{CH} , 927.43, 798.32, 787.16. HRMS (ESI) m/z calcd for $\text{C}_{22}\text{H}_{22}\text{ClN}_2\text{O}_3$ [$\text{M} + \text{H}$] $^+$: 397.1313, found 397.1317.

5-[2,3-Dimethyl-4-(2-methylene-1-oxopropyl)phenoxyethyl]-3-(4-nitrobenzyl)-1,2,4-oxadiazol (6m). White powder, yield 38.0%, mp 114.8–115.6 °C, TLC $R_f = 0.39$ (acetone/petroleum ether, 1:3, v/v). ^1H NMR (CDCl_3) δ (ppm): 8.20 (d, $J = 9.00$ Hz, 2H), 7.51 (d, $J = 8.40$ Hz, 2H), 7.05 (d, $J = 8.40$ Hz, 1H), 6.71 (d, $J = 8.40$ Hz, 1H), 5.94 (s, 1H), 5.55 (s, 1H), 5.28 (s, 2H), 4.22 (s, 2H), 2.21 (s, 3H), 2.18 (s, 3H), 2.04 (s, 3H). ^{13}C NMR (CDCl_3) δ (ppm): 200.66, 175.31, 168.46, 156.18, 145.52, 142.36, 136.92, 134.08, 129.99, 129.76, 126.98, 126.23, 123.97, 108.04, 61.40, 32.04, 17.35, 17.17, 11.78. IR (KBr, cm^{-1}): ν_{CH} , 3101.26; ν_{CH} , 2982.54, 2922.70; $\nu_{\text{C=O}}$, 1644.24; $\nu_{\text{C=C}}$, 1624.18, 1579.31; ν_{NO_2} , 1591.73, 1366.14; δ_{CH} , 1491.34, 1448.69, 1375.08; $\nu_{\text{C-O}}$, 1265.04, 1096.70; γ_{CH} , 927.36, 798.31, 787.21. HRMS (ESI) m/z calcd for $\text{C}_{22}\text{H}_{22}\text{N}_3\text{O}_5$ [$\text{M} + \text{H}$] $^+$: 408.1554, found 408.1558.

5-[3-Chloro-4-(2-methylene-1-oxopropyl)phenoxyethyl]-3-methyl-1,2,4-oxadiazole (6n). Yellowish oil, yield 20.5%, TLC $R_f = 0.40$ (acetone/petroleum ether, 1:3, v/v). ^1H NMR (CDCl_3) δ (ppm): 7.26 (d, $J = 8.40$ Hz, 1H), 7.04 (s, 1H), 6.91 (d, $J = 8.40$ Hz, 1H), 5.98 (s, 1H), 5.58 (s, 1H), 5.29 (s, 2H), 2.45 (s, 3H), 2.04 (s, 3H). IR (KBr, cm^{-1}): ν_{CH} , 3088.06; ν_{CH} , 2980.30, 2926.79; $\nu_{\text{C=O}}$, 1664.71; $\nu_{\text{C=C}}$, 1599.58; $\nu_{\text{C-O}}$, 1228.90; γ_{CH_2} , 1060.84. HRMS (ESI) m/z calcd for $\text{C}_{14}\text{H}_{14}\text{ClN}_2\text{O}_3$ [$\text{M} + \text{H}$] $^+$: 293.0474, found 293.0479.

5-[3-Chloro-4-(2-methylene-1-oxopropyl)phenoxyethyl]-3-phenyl-1,2,4-oxadiazole (6o). White powder, yield 55.3%, mp 56.2–57.2 °C, TLC $R_f = 0.55$ (acetone/petroleum ether, 1:3, v/v). ^1H NMR (CDCl_3) δ (ppm): 8.10 (m, 2H), 7.51 (m, 3H), 7.27 (d, $J = 8.40$ Hz, 1H), 7.10 (d, $J = 2.40$ Hz, 1H), 6.96 (dd, $J_1 = 8.40$ Hz, $J_2 = 2.40$ Hz, 1H), 5.98 (s, 1H), 5.59 (s, 1H), 5.38 (s, 2H), 2.04 (s, 3H). IR (KBr, cm^{-1}): ν_{CH} , 3071.14; ν_{CH} , 2924.87; $\nu_{\text{C=O}}$, 1664.10; $\nu_{\text{C=C}}$, 1599.61; $\nu_{\text{C-O}}$, 1229.05; γ_{CH_2} , 1060.09, 721.03. HRMS (ESI) m/z calcd for $\text{C}_{19}\text{H}_{16}\text{ClN}_2\text{O}_3$ [$\text{M} + \text{H}$] $^+$: 355.0844, found 355.0850.

5-[3-Chloro-4-(2-methylene-1-oxopropyl)phenoxyethyl]-3-(4-fluorophenyl)-1,2,4-oxadiazol (6p). White powder, yield 56.8%, mp 78.9–79.5 °C, TLC $R_f = 0.34$ (acetone/petroleum ether, 1:3, v/v). ^1H NMR (CDCl_3) δ (ppm): 8.10 (m, 2H), 7.28 (m, 1H), 7.19 (m, 2H), 7.10 (m, 1H), 6.97 (m, 1H), 5.99 (s, 1H), 5.59 (s, 1H), 5.37 (s, 2H), 2.04 (s, 3H). ^{13}C NMR (CDCl_3) δ (ppm): 196.64, 173.92, 167.88, 164.78 (d, $J_{\text{C-F}} = 250.80$ Hz), 158.72, 144.63, 132.80, 132.77, 130.37, 130.12, 129.76 (d, $J_{\text{C-F}} = 9.44$ Hz), 122.37 (d, $J_{\text{C-F}} = 3.15$ Hz), 116.54, 116.21 (d, $J_{\text{C-F}} = 21.75$ Hz), 112.86, 61.13, 17.06. IR (KBr, cm^{-1}): ν_{CH} , 3084.41; ν_{CH} , 2963.53, 2917.41; $\nu_{\text{C=O}}$, 1651.03; $\nu_{\text{C=C}}$, 1609.08, 1597.38, 1587.12; δ_{CH} , 1482.76, 1419.08, 1359.67; $\nu_{\text{C-O}}$, 1234.81, 1055.99; γ_{CH} , 917.50, 843.18, 749.66. HRMS (ESI) m/z calcd for $\text{C}_{19}\text{H}_{15}\text{ClFN}_2\text{O}_3$ [$\text{M} + \text{H}$] $^+$: 373.0750, found 373.0734.

5-[3-Chloro-4-(2-methylene-1-oxopropyl)phenoxyethyl]-3-(4-trifluoromethylphenyl)-1,2,4-oxadiazol (6q). White powder, yield 46.6%, mp 86.7–87.2 °C, TLC $R_f = 0.32$ (acetone/petroleum ether, 1:3, v/v). ^1H NMR (CDCl_3) δ (ppm): 8.23 (d, $J = 7.80$ Hz, 2H), 7.77 (d, $J = 8.40$ Hz, 2H), 7.28 (m, 1H), 7.10 (m, 1H), 6.97 (m, 1H), 5.99 (s, 1H), 5.59 (s, 1H), 5.40 (s, 2H), 2.04 (s, 3H). ^{13}C NMR (CDCl_3) δ (ppm): 196.63, 174.40, 167.72, 158.65, 144.64, 133.39, 133.17, 132.89, 132.80, 130.40, 130.16, 129.51, 127.95, 125.99 (q, $J_{\text{C-F}} = 3.75$ Hz), 116.54, 112.87, 61.12, 17.06. IR (KBr, cm^{-1}): ν_{CH} , 3082.30; ν_{CH} , 2929.58; $\nu_{\text{C=O}}$, 1646.25; $\nu_{\text{C=C}}$, 1624.55, 1597.35, 1561.72; δ_{CH} , 1490.25, 1444.04, 1324.81; $\nu_{\text{C-O}}$, 1228.19, 1065.21; γ_{CH} , 853.57, 717.77. HRMS (ESI) m/z calcd for $\text{C}_{20}\text{H}_{15}\text{ClF}_3\text{N}_2\text{O}_3$ [$\text{M} + \text{H}$] $^+$: 423.0718, found 423.0706.

5-[2,3-Dichloro-4-(2-methylene-1-oxobutyl)phenoxyethyl]-3-methyl-1,2,4-oxadiazole (6r). White powder, yield 52.9%, mp 78.5–79.4 °C, TLC $R_f = 0.37$ (acetone/petroleum ether, 1:3, v/v). ^1H NMR (CDCl_3) δ (ppm): 7.15 (d, $J = 8.40$ Hz, 1H), 6.96 (d, $J = 8.40$ Hz, 1H), 5.96 (s, 1H), 5.60 (s, 1H), 5.38 (s, 2H), 2.47 (q, $J = 7.80$ Hz, 2H), 2.45 (s, 3H), 1.15 (t, $J = 7.20$ Hz, 3H). ^{13}C NMR (CDCl_3) δ (ppm): 195.89, 173.49, 167.84, 155.16, 150.30, 129.09, 127.03, 111.55, 62.28, 23.58, 12.59, 11.80. IR (KBr, cm^{-1}): ν_{CH} , 3104.30; ν_{CH} , 2970.72, 2945.48, 2883.28; $\nu_{\text{C=O}}$, 1667.98; $\nu_{\text{C=C}}$, 1599.02; $\nu_{\text{C-O}}$, 1278.91; γ_{CH_2} , 1063.05, 802.53. HRMS (ESI) m/z calcd for $\text{C}_{15}\text{H}_{15}\text{Cl}_2\text{N}_2\text{O}_3$ [$\text{M} + \text{H}$] $^+$: 341.0454, found 341.0461.

5-[2,3-Dichloro-4-(2-methylene-1-oxobutyl)phenoxyethyl]-3-phenyl-1,2,4-oxadiazole (6s). White powder, yield 67.2%, mp 93.2–93.8 °C, TLC $R_f = 0.45$ (acetone/petroleum ether, 1:3, v/v). ^1H NMR (CDCl_3) δ (ppm): 8.09 (m, 2H), 7.52 (m, 3H), 7.16 (d, $J = 8.40$ Hz, 1H), 7.03 (d, $J = 8.40$ Hz, 1H), 5.95 (s, 1H), 5.60 (s, 1H), 5.47 (s, 2H), 2.45 (q, $J = 7.20$ Hz, 2H), 1.14 (t, $J = 7.20$ Hz, 3H). ^{13}C NMR (CDCl_3) δ (ppm): 195.68, 173.52, 168.68, 155.02, 150.07, 134.63, 131.67, 131.61, 128.97, 128.90, 127.54, 126.84, 126.05, 111.48, 62.21, 23.36, 12.37. IR (KBr, cm^{-1}): ν_{CH} , 3084.65; ν_{CH} , 2969.39, 2938.28; $\nu_{\text{C=O}}$, 1670.22; $\nu_{\text{C=C}}$, 1586.23; $\nu_{\text{C-O}}$, 1281.15; γ_{CH_2} , 1070.47, 722.22. HRMS (ESI) m/z calcd for $\text{C}_{20}\text{H}_{17}\text{Cl}_2\text{N}_2\text{O}_3$ [$\text{M} + \text{H}$] $^+$: 403.0611, found 403.0617.

5-[2,3-Dichloro-4-(2-methylene-1-oxobutyl)phenoxyethyl]-3-(4-fluorophenyl)-1,2,4-oxadiazol (6t). White powder, yield 44.5%, mp 94.6–95.4 °C, TLC $R_f = 0.48$ (acetone/petroleum ether, 1:3, v/v). ^1H NMR (CDCl_3) δ (ppm): 8.10 (m, 2H), 7.16 (m, 3H), 7.04 (d, $J = 9.00$ Hz, 1H), 5.96 (s, 1H), 5.60 (s, 1H), 5.47 (s, 2H), 2.47 (q, $J = 7.40$ Hz, 2H), 1.15 (t, $J = 7.50$ Hz, 3H). ^{13}C NMR (CDCl_3) δ (ppm): 195.65, 173.65, 167.90, 164.79 (d, $J_{\text{C-F}} = 251.10$ Hz), 155.01, 150.12, 134.74, 131.72, 129.77 (d, $J_{\text{C-F}} = 9.15$ Hz), 128.85, 126.84, 123.88, 122.31, 116.22 (d, $J_{\text{C-F}} = 21.75$ Hz), 111.52, 62.21, 23.38, 12.38. IR (KBr, cm^{-1}): ν_{CH} , 3079.94; ν_{CH} , 2971.08, 2942.01; $\nu_{\text{C=O}}$, 1667.37; $\nu_{\text{C=C}}$, 1606.97, 1596.92, 1584.78; δ_{CH} , 1484.99, 1467.65, 1385.17; $\nu_{\text{C-O}}$, 1278.69, 1048.64; γ_{CH} , 912.48, 849.06, 755.82. HRMS (ESI) m/z calcd for $\text{C}_{20}\text{H}_{16}\text{Cl}_2\text{FN}_2\text{O}_3$ [$\text{M} + \text{H}$] $^+$: 421.0517, found 421.0523.

5-[2,3-Dichloro-4-(2-methylene-1-oxobutyl)phenoxyethyl]-3-(4-trifluoromethylphenyl)-1,2,4-oxadiazol (6u). White powder, yield 51.8%, mp 121.2–121.9 °C, TLC $R_f = 0.46$ (acetone/petroleum ether, 1:3, v/v). ^1H NMR (CDCl_3) δ (ppm): 8.23 (d, $J = 8.40$ Hz, 2H), 7.77 (d, $J = 7.80$ Hz, 2H), 7.18 (d, $J = 9.00$ Hz, 1H), 7.04 (d, $J = 8.40$ Hz, 1H), 5.96 (s, 1H), 5.60 (s, 1H), 5.50 (s, 2H), 2.47 (q, $J = 7.40$ Hz, 2H), 1.15 (t, $J = 7.50$ Hz, 3H). ^{13}C NMR (CDCl_3) δ (ppm): 195.63, 174.08, 167.73, 154.95, 150.11, 134.82, 131.76, 129.48, 128.91, 127.95, 126.86, 125.99 (q, $J_{\text{C-F}} = 3.80$ Hz), 124.58, 123.90, 122.77, 111.54, 62.20, 23.38, 12.38. IR (KBr, cm^{-1}): ν_{CH} , 3084.58; ν_{CH} , 2974.95, 2936.48, 2879.35; $\nu_{\text{C=O}}$, 1661.10; $\nu_{\text{C=C}}$, 1623.11, 1603.46, 1585.57; δ_{CH} , 1471.07, 1421.92, 1328.83; $\nu_{\text{C-O}}$, 1169.28, 1065.62; γ_{CH} , 856.46, 802.50, 758.93. HRMS (ESI) m/z calcd for $\text{C}_{21}\text{H}_{16}\text{Cl}_2\text{F}_3\text{N}_2\text{O}_3$ [$\text{M} + \text{H}$] $^+$: 471.0485, found 471.0487.

5-[2,3-Dichloro-4-(2-methylene-1-oxobutyl)phenoxyethyl]-3-(4-methoxyphenyl)-1,2,4-oxadiazol (6v). White powder, yield 48.6%, mp 87.6–88.1 °C, TLC $R_f = 0.40$ (acetone/petroleum

ether, 1:3, v/v). $^1\text{H NMR}$ (CDCl_3) δ (ppm): 8.03 (d, $J = 8.40$ Hz, 2H), 7.17 (d, $J = 9.00$ Hz, 1H), 7.04 (d, $J = 8.40$ Hz, 1H), 7.00 (d, $J = 9.00$ Hz, 2H), 5.95 (s, 1H), 5.60 (s, 1H), 5.45 (s, 2H), 3.87 (s, 3H), 2.47 (q, $J = 7.40$ Hz, 2H), 1.15 (t, $J = 7.50$ Hz, 3H). $^{13}\text{C NMR}$ (CDCl_3) δ (ppm): 195.64, 173.19, 168.36, 162.19, 155.04, 150.07, 134.58, 131.63, 129.17, 128.82, 126.82, 123.79, 118.45, 114.33, 111.47, 62.21, 55.39, 23.35, 12.36. IR (KBr, cm^{-1}): ν_{CH} , 2967.20, 2937.32, 2873.93, 2839.76; $\nu_{\text{C=O}}$, 1662.69; $\nu_{\text{C=C}}$, 1610.68, 1597.01, 1585.31; δ_{CH} , 1481.95, 1472.74, 1360.51; $\nu_{\text{C-O}}$, 1260.62, 1065.35; γ_{CH} , 910.38, 846.54, 755.24. HRMS (ESI) m/z calcd for $\text{C}_{21}\text{H}_{19}\text{Cl}_2\text{N}_2\text{O}_4$ [$\text{M} + \text{H}$] $^+$: 433.0716, found 433.0721.

5-[2,3-Dichloro-4-(2-methylene-1-oxobutyl)phenoxyethyl]-3-(4-chlorobenzyl)-1,2,4-oxadiazol (6w). White powder, yield 54.7%, mp 57.7–58.3 °C, TLC $R_f = 0.40$ (acetone/petroleum ether, 1:3, v/v). $^1\text{H NMR}$ (CDCl_3) δ (ppm): 7.30 (d, $J = 8.40$ Hz, 2H), 7.25 (d, $J = 8.40$ Hz, 2H), 7.13 (d, $J = 8.40$ Hz, 1H), 6.94 (d, $J = 9.00$ Hz, 1H), 5.96 (s, 1H), 5.58 (s, 1H), 5.36 (s, 2H), 4.08 (s, 2H), 2.47 (q, $J = 7.40$ Hz, 2H), 1.15 (t, $J = 7.60$ Hz, 3H). $^{13}\text{C NMR}$ (CDCl_3) δ (ppm): 195.62, 173.74, 169.47, 154.90, 150.08, 134.69, 133.36, 133.30, 131.65, 130.37, 128.94, 128.88, 126.77, 123.85, 111.53, 62.18, 31.58, 23.36, 12.38. IR (KBr, cm^{-1}): ν_{CH} , 3086.99; ν_{CH} , 2970.79, 2933.93, 2876.00; $\nu_{\text{C=O}}$, 1661.23; $\nu_{\text{C=C}}$, 1619.26, 1585.62; δ_{CH} , 1492.16, 1468.85, 1382.35; $\nu_{\text{C-O}}$, 1287.26, 1037.36; γ_{CH} , 945.48, 802.96, 751.57. HRMS (ESI) m/z calcd for $\text{C}_{21}\text{H}_{18}\text{Cl}_3\text{N}_2\text{O}_3$ [$\text{M} + \text{H}$] $^+$: 451.0378, found 451.0382.

5-[2,3-Dichloro-4-(2-methylene-1-oxobutyl)phenoxyethyl]-3-(4-nitrobenzyl)-1,2,4-oxadiazol (6x). White powder, yield 60.4%, mp 67.9–68.8 °C, TLC $R_f = 0.40$ (acetone/petroleum ether, 1:3, v/v). $^1\text{H NMR}$ (CDCl_3) δ (ppm): 8.20 (d, $J = 7.80$ Hz, 2H), 7.51 (d, $J = 7.80$ Hz, 2H), 7.14 (d, $J = 7.80$ Hz, 1H), 6.96 (d, $J = 8.40$ Hz, 1H), 5.96 (s, 1H), 5.78 (s, 1H), 5.38 (s, 2H), 4.23 (s, 2H), 2.47 (q, $J = 6.60$ Hz, 2H), 1.15 (t, $J = 6.90$ Hz, 3H). $^{13}\text{C NMR}$ (CDCl_3) δ (ppm): 195.58, 174.10, 168.65, 154.86, 150.12, 147.32, 142.22, 134.83, 131.70, 130.02, 128.87, 126.78, 123.99, 123.91, 111.58, 62.18, 32.02, 23.36, 12.38. IR (KBr, cm^{-1}): ν_{CH} , 3083.36; ν_{CH} , 2974.62, 2937.10, 2876.43; $\nu_{\text{C=O}}$, 1658.64; ν_{NO_2} , 1528.05, 1348.95; $\nu_{\text{C=C}}$, 1608.29, 1594.37, 1585.54; δ_{CH} , 1469.26, 1427.81, 1378.71; $\nu_{\text{C-O}}$, 1266.53, 1040.13; γ_{CH} , 803.73, 721.79. HRMS (ESI) m/z calcd for $\text{C}_{21}\text{H}_{18}\text{Cl}_2\text{N}_3\text{O}_5$ [$\text{M} + \text{H}$] $^+$: 462.0618, found 462.0624.

5-[3-Bromo-4-(2-methylene-1-oxopropyl)phenoxyethyl]-3-methyl-1,2,4-oxadiazole (6y). White powder, yield 38.6%, mp 63.5–64.5 °C, TLC $R_f = 0.45$ (acetone/petroleum ether, 1:3, v/v). $^1\text{H NMR}$ (CDCl_3) δ (ppm): 7.23 (m, 2H), 6.96 (dd, $J_1 = 8.40$ Hz, $J_2 = 2.40$ Hz, 1H), 5.99 (s, 1H), 5.57 (s, 1H), 5.28 (s, 2H), 2.45 (s, 3H), 2.04 (s, 3H). IR (KBr, cm^{-1}): ν_{CH} , 3087.83; ν_{CH} , 2979.57, 2925.71; $\nu_{\text{C=O}}$, 1664.55; $\nu_{\text{C=C}}$, 1596.68; $\nu_{\text{C-O}}$, 1225.30; γ_{CH_2} , 1050.30. HRMS (ESI) m/z calcd for $\text{C}_{14}\text{H}_{14}\text{BrN}_2\text{O}_3$ [$\text{M} + \text{H}$] $^+$: 337.0182, found 337.0187.

5-[3-Bromo-4-(2-methylene-1-oxopropyl)phenoxyethyl]-3-phenyl-1,2,4-oxadiazole (6z). White powder, yield 45.1%, mp 52.3–53.5 °C, TLC $R_f = 0.51$ (acetone/petroleum ether, 1:3, v/v). $^1\text{H NMR}$ (CDCl_3) δ (ppm): 8.09 (d, $J = 6.60$ Hz, 2H), 7.51 (m, 3H), 7.29 (s, 1H), 7.24 (s, 1H), 7.01 (d, $J = 8.40$ Hz, 1H), 5.99 (s, 1H), 5.58 (s, 1H), 5.38 (s, 2H), 2.05 (s, 3H). IR (KBr, cm^{-1}): ν_{CH} , 3070.23; ν_{CH} , 2979.31, 2924.44; $\nu_{\text{C=O}}$, 1664.13; $\nu_{\text{C=C}}$, 1596.64; $\nu_{\text{C-O}}$, 1225.52; γ_{CH_2} , 1048.82, 720.90. HRMS (ESI) m/z calcd for $\text{C}_{19}\text{H}_{16}\text{BrFN}_2\text{O}_3$ [$\text{M} + \text{H}$] $^+$: 399.0339, found 399.0345.

5-[3-Bromo-4-(2-methylene-1-oxopropyl)phenoxyethyl]-3-(4-fluorophenyl)-1,2,4-oxadiazol (6aa). White powder, yield 42.3%, mp 83.5–84.5 °C, TLC $R_f = 0.32$ (acetone/petroleum ether, 1:3, v/v). $^1\text{H NMR}$ (CDCl_3) δ (ppm): 8.10 (m, 2H), 7.28 (s, 1H), 7.25 (d, $J = 8.40$ Hz, 1H), 7.18 (m, 2H), 7.01 (d, $J = 8.40$ Hz, 1H), 5.99 (s, 1H), 5.58 (s, 1H), 5.37 (s, 2H), 2.05 (s, 3H). $^{13}\text{C NMR}$ (CDCl_3) δ (ppm): 197.37, 173.97, 167.85, 164.75 (d, $J_{\text{C-F}} = 250.50$ Hz), 158.50, 144.35, 134.81, 130.46, 130.12, 129.75 (d, $J_{\text{C-F}} = 9.15$ Hz), 122.36 (d, $J_{\text{C-F}} = 2.85$ Hz), 119.62,

116.27, 116.20 (d, $J_{\text{C-F}} = 21.75$ Hz), 113.35, 61.13, 17.07. IR (KBr, cm^{-1}): ν_{CH} , 3084.06; ν_{CH} , 2961.47, 2918.03; $\nu_{\text{C=O}}$, 1652.06; $\nu_{\text{C=C}}$, 1626.31, 1607.83, 1596.43; δ_{CH} , 1483.47, 1417.55, 1360.58; $\nu_{\text{C-O}}$, 1233.89, 1049.56; γ_{CH} , 909.40, 843.84, 749.64. HRMS (ESI) m/z calcd for $\text{C}_{19}\text{H}_{15}\text{BrFN}_2\text{O}_3$ [$\text{M} + \text{H}$] $^+$: 417.0245, found 417.0250.

5-[3-Bromo-4-(2-methylene-1-oxopropyl)phenoxyethyl]-3-(4-trifluoromethylphenyl)-1,2,4-oxadiazol (6ab). White powder, yield 55.2%, mp 104.7–105.5 °C, TLC $R_f = 0.32$ (acetone/petroleum ether, 1:3, v/v). $^1\text{H NMR}$ (CDCl_3) δ (ppm): 8.24 (d, $J = 8.40$ Hz, 2H), 7.77 (d, $J = 8.40$ Hz, 2H), 7.29 (d, $J = 8.40$ Hz, 1H), 7.25 (s, 1H), 7.02 (d, $J = 9.00$ Hz, 1H), 6.00 (s, 1H), 5.58 (s, 1H), 5.40 (s, 2H), 2.05 (s, 3H). $^{13}\text{C NMR}$ (CDCl_3) δ (ppm): 197.35, 174.40, 167.73, 158.46, 144.39, 134.96, 133.18, 130.46, 130.43, 130.15, 129.52, 127.95, 125.98 (q, $J_{\text{C-F}} = 3.75$ Hz), 120.74, 119.64, 113.39, 61.14, 17.07. IR (KBr, cm^{-1}): ν_{CH} , 3078.22; ν_{CH} , 2929.49; $\nu_{\text{C=O}}$, 1643.72; $\nu_{\text{C=C}}$, 1624.33, 1594.17; δ_{CH} , 1487.87, 1443.20, 1325.04; $\nu_{\text{C-O}}$, 1226.80, 1136.00; γ_{CH} , 853.19, 717.72. HRMS (ESI) m/z calcd for $\text{C}_{20}\text{H}_{15}\text{BrF}_3\text{N}_2\text{O}_3$ [$\text{M} + \text{H}$] $^+$: 467.0217, found 467.0213.

Biological Activity Methods. Cell Lines. HL-60, PC-3, and DU-145 cells were cultured in RPMI-1640 medium supplemented with 100 U/mL penicillin, 100 $\mu\text{g}/\text{mL}$ streptomycin, 1 mmol/L L-glutamine, and 10% (v/v) heat-inactivated fetal bovine serum (FBS). T47D and MDA-MB-231 cells were cultured in RPMI 1640 medium supplemented with 10% FBS, 5 $\mu\text{g}/\text{mL}$ insulin, 100 U/mL penicillin, and 100 $\mu\text{g}/\text{mL}$ streptomycin. MCF-7 cells were cultured in DMEM medium supplemented with 10% FBS, 5 $\mu\text{g}/\text{mL}$ insulin, 100 U/mL penicillin, and 100 $\mu\text{g}/\text{mL}$ streptomycin. MCF-10A cells were maintained in DMEM/F12 supplemented with 5% donor horse serum, 20 ng/mL epidermal growth factor (EGF), 10 $\mu\text{g}/\text{mL}$ insulin, 1 ng/mL cholera toxin, 100 $\mu\text{g}/\text{mL}$ hydrocortisone, 50 U/mL penicillin, and 50 $\mu\text{g}/\text{mL}$ streptomycin.

GST P1-1 Activity Assay. GST P1-1 activity was measured spectrophotometrically at 25 °C using 1-chloro-2,4-dinitrobenzene (CDNB) and GSH as substrates as described before.¹⁷ The CDNB-GSH product has a strong molar absorptivity at 340 nm, and the extinction coefficient of 9.6 $\text{mM}^{-1}\text{cm}^{-1}$ was used to calculate GST P1-1 activity. GST P1-1 activity was expressed as nanomoles of product per minute per milligram of protein. The percent inhibition rates were calculated as $[(V_c - V_t)/V_c] \times 100$. V_c represents GST P1-1 activity of the control group, and V_t represents GST P1-1 activity of the treated group. The concentration of the tested compound that inhibits 50% of GST P1-1 activity (IC_{50}) was calculated.

Cell Proliferation Inhibition of HL-60 Cells. Cell proliferation was determined as reported previously.¹⁸ Cells were plated in 12-well microplates at a density of 1×10^5 cells/mL and incubated with various concentrations of the test compounds. Cell number in each group was counted with the aid of a hemocytometer. The percent cell growth inhibition rate was calculated as $[(N_c - N_t)/N_c] \times 100$. N_c represents the cell number of the control group, and N_t represents the cell number of the treated group. The concentration inhibiting 50% of the cell proliferation (GI_{50}) was calculated.

3-(4,5-Dimethylthiazol-2-yl)-2,5-diphenyltetrazolium Bromide (MTT) Assay. PC-3, DU-145, T47D, MCF-7, MDA-MB-231, and MCF 10A cells (2×10^3) were plated in each well of a 96-well plate and allowed to adhere and spread for 24 h. Then various concentrations (20, 10, 5, 2.5, 1.25, 0.625, and 0 μM) of **6r** and **6s** were added, and then the cells were cultured for 4 days at 37 °C. MTT solution (50 μL of 2 mg/mL) was added per well, and the cultures were continued for an additional 4 h. The medium was aspirated, the cells were dissolved in 200 μL of DMSO, and the optical density (OD) at 570 nm was determined in each well with a 96-well plate reader. The percent cell growth inhibition rate was calculated as $[(\text{OD}_c - \text{OD}_t)/\text{OD}_c] \times 100$. OD_c represents the OD of the control group, and OD_t represents the OD of the

treated group. The concentration inhibiting 50% of the cell proliferation (GI₅₀) was calculated.

Acknowledgment. This work was supported by grants from the National Natural Science Foundation of China (Grant No. 20672069) and Major Projects of Science and Technology for Drug Innovation (Grant No. 2009ZX09103-116).

Supporting Information Available: Purity data for all tested compounds and the methods for HPLC analysis. This material is available free of charge via the Internet at <http://pubs.acs.org>.

References

- Townsend, D. M.; Tew, K. D. The role of glutathione-*S*-transferase in anti-cancer drug resistance. *Oncogene* **2003**, *22*, 7369–7375.
- Goto, S.; Iida, T.; Cho, S.; Oka, M.; Kohno, S.; Kondo, T. Overexpression of glutathione *S*-transferase pi enhances the adduct formation of cisplatin with glutathione in human cancer cells. *Free Radical Res.* **1999**, *31*, 549–558.
- Cazenave, L. A.; Moscow, J. A.; Myers, C. E.; Cowan, K. H. Glutathione *S*-transferase and drug resistance. *Cancer Treat. Res.* **1989**, *48*, 171–187.
- Shen, H.; Kauvar, L.; Tew, K. D. Importance of glutathione and associated enzymes in drug response. *Oncol. Res.* **1997**, *9*, 295–302.
- Zhou, L.; Jing, Y.; Styblo, M.; Chen, Z.; Waxman, S. Glutathione-*S*-transferase pi inhibits As2O₃-induced apoptosis in lymphoma cells: involvement of hydrogen peroxide catabolism. *Blood* **2005**, *105*, 1198–1203.
- Yin, Z.; Ivanov, V. N.; Habelhah, H.; Tew, K.; Ronai, Z. Glutathione *S*-transferase p elicits protection against H₂O₂-induced cell death via coordinated regulation of stress kinases. *Cancer Res.* **2000**, *60*, 4053–4057.
- Adler, V.; Yin, Z.; Fuchs, S. Y.; Benezra, M.; Rosario, L.; Tew, K. D.; Pincus, M. R.; Sardana, M.; Henderson, C. J.; Wolf, C. R.; Davis, R. J.; Ronai, Z. Regulation of JNK signaling by GSTp. *EMBO J.* **1999**, *18*, 1321–1334.
- Wang, T.; Arifoglu, P.; Ronai, Z.; Tew, K. D. Glutathione *S*-transferase P1-1 (GSTP1-1) inhibits c-Jun N-terminal kinase (JNK1) signaling through interaction with the C terminus. *J. Biol. Chem.* **2001**, *276*, 20999–21003.
- Gate, L.; Tew, K. D. Glutathione *S*-transferases as emerging therapeutic targets. *Expert Opin. Ther. Targets* **2001**, *5*, 477–489.
- Mahajan, S. S.; Hou, L.; Doneanu, C.; Paranj, R.; Maeda, D.; Zebala, J.; Atkins, W. M. Optimization of bivalent glutathione *S*-transferase inhibitors by combinatorial linker design. *J. Am. Chem. Soc.* **2006**, *128*, 8615–8625.
- Tew, K. D.; Dutta, S.; Schultz, M. Inhibitors of glutathione *S*-transferases as therapeutic agents. *Adv. Drug Delivery Rev.* **1997**, *26*, 91–104.
- Iersel, M. L.; Ploemen, J. P.; Struik, I.; van Amersfoort, C.; Keyzer, A. E.; Schefferlie, J. G.; van Bladeren, P. J. Inhibition of glutathione *S*-transferase activity in human melanoma cells by alpha,beta-unsaturated carbonyl derivatives. Effects of acrolein, cinnamaldehyde, citral, crotonaldehyde, curcumin, ethacrynic acid, and *trans*-2-hexenal. *Chem.-Biol. Interact.* **1996**, *102*, 117–132.
- Aizawa, S.; Ookawa, K.; Kudo, T.; Asano, J.; Hayakari, M.; Tsuchida, S. Characterization of cell death induced by ethacrynic acid in a human colon cancer cell line DLD-1 and suppression by *N*-acetyl-L-cysteine. *Cancer Sci.* **2003**, *94*, 886–893.
- Zhao, G.; Wang, X. Advance in antitumor agents targeting glutathione-*S*-transferase. *Curr. Med. Chem.* **2006**, *13*, 1461–1471.
- O'Dwyer, P. J.; LaCreta, F.; Nash, S.; Tinsley, P. W.; Schilder, R.; Clapper, M. L.; Tew, K. D.; Panting, L.; Litwin, S.; Comis, R. L.; et al. Phase I study of thiotepa in combination with the glutathione transferase inhibitor ethacrynic acid. *Cancer Res.* **1991**, *51*, 6059–6065.
- van Iersel, M. L.; van Lipzig, M. M.; Rietjens, I. M.; Vervoort, J.; van Bladeren, P. J. GSTP1-1 stereospecifically catalyzes glutathione conjugation of ethacrynic acid. *FEBS Lett.* **1998**, *441*, 153–157.
- Zhao, G.; Yu, T.; Wang, R.; Wang, X.; Jing, Y. Synthesis and structure–activity relationship of ethacrynic acid analogues on glutathione-*S*-transferase P1-1 activity inhibition. *Bioorg. Med. Chem.* **2005**, *13*, 4056–4062.
- Zhao, G.; Liu, C.; Wang, R.; Song, D.; Wang, X.; Lou, H.; Jing, Y. The synthesis of alpha,beta-unsaturated carbonyl derivatives with the ability to inhibit both glutathione *S*-transferase P1-1 activity and the proliferation of leukemia cells. *Bioorg. Med. Chem.* **2007**, *15*, 2701–2707.
- Wang, R.; Li, C.; Song, D.; Zhao, G.; Zhao, L.; Jing, Y. Ethacrynic acid butyl-ester induces apoptosis in leukemia cells through a hydrogen peroxide mediated pathway independent of glutathione *S*-transferase P1-1 inhibition. *Cancer Res.* **2007**, *67*, 7856–7864.
- Lima, L. M.; Barreiro, E. J. Bioisosterism: a useful strategy for molecular modification and drug design. *Curr. Med. Chem.* **2005**, *12*, 23–49.
- Schultz, E. M.; Sprague, J. M. (2-Alkylidene acyl)phenoxy- and (2-Alkylidene acyl)phenylmercaptocarboxylic Acids. U.S. Patent 3255241, June 7, 1966.
- Sasse, A.; Sadek, B.; Ligneau, X.; Elz, S.; Pertz, H. H.; Luger, P.; Ganellin, C. R.; Arrang, J. M.; Schwartz, J. C.; Schunack, W.; Stark, H. New histamine H(3)-receptor ligands of the proxifan series: imoproxifan and other selective antagonists with high oral in vivo potency. *J. Med. Chem.* **2000**, *43*, 3335–3343.
- Chiou, S.; Shine, H. J. A simplified procedure for preparing 3, 5-disubstituted-1,2,4-oxadiazoles by reaction of amidoximes with acyl chlorides in pyridine solution. *J. Heterocycl. Chem.* **1989**, *26*, 125–128.
- Oakley, A. J.; Rossjohn, J.; Lo Bello, M.; Caccuri, A. M.; Federici, G.; Parker, M. W. The three-dimensional structure of the human pi class glutathione transferase P1-1 in complex with the inhibitor ethacrynic acid and its glutathione conjugate. *Biochemistry* **1997**, *36*, 576–585.
- Oakley, A. J.; Lo Bello, M.; Mazzetti, A. P.; Federici, G.; Parker, M. W. The glutathione conjugate of ethacrynic acid can bind to human pi class glutathione transferase P1-1 in two different modes. *FEBS Lett.* **1997**, *419*, 32–36.
- Awasthi, S.; Srivastava, S. K.; Ahmad, F.; Ahmad, H.; Ansari, G. A. Interactions of glutathione-*S*-transferase-pi with ethacrynic acid and its glutathione conjugate. *Biochim. Biophys. Acta* **1993**, *1164*, 173–178.
- Voehringer, D. W. BCL-2 and glutathione: alterations in cellular redox state that regulate apoptosis sensitivity. *Free Radical Biol. Med.* **1999**, *27*, 945–950.
- Hall, A. G. Review: The role of glutathione in the regulation of apoptosis. *Eur. J. Clin. Invest.* **1999**, *29*, 238–245.
- Han, Y.; Englert, J. A.; Delude, R. L.; Fink, M. P. Ethacrynic acid inhibits multiple steps in the NF-kappaB signaling pathway. *Shock* **2005**, *23*, 45–53.
- Jin, G.; Lu, D.; Yao, S.; Wu, C. C.; Liu, J. X.; Carson, D. A.; Cottam, H. B. Amide derivatives of ethacrynic acid: synthesis and evaluation as antagonists of Wnt/beta-catenin signaling and CLL cell survival. *Bioorg. Med. Chem. Lett.* **2009**, *19*, 606–609.